Energy levels of ^{249}Bk populated in the α decay of $^{253}_{99}$Es and β^- decay of $^{249}_{96}$Cm

I. Ahmad, F. G. Kondev, E. F. Moore, M. P. Carpenter, R. R. Chasman, J. P. Greene, R. V. F. Janssens,
T. Lauritsen, C. J. Lister, and D. Seweryniak

Argonne National Laboratory, Argonne, Illinois 60439, USA

R. W. Hoff, J. E. Evans, and R. W. Lougheed

Lawrence Livermore National Laboratory, Livermore, California 94551, USA

C. E. Porter and L. K. Felker

Nuclear Science and Technology Division, Oak Ridge National Laboratory, Oak Ridge, Tennessee 37831, USA

The level structure of ^{249}Bk has been investigated by measuring the γ-ray spectra of an extremely pure ^{253}Es sample obtained by milking this nuclide from ^{253}Cf source material produced in the High Flux Isotope Reactor at Oak Ridge National Laboratory. Additional information on the ^{249}Bk levels was obtained from the β^--decay study of ^{249}Cm, produced by neutron irradiation of ^{248}Cm. Using the results of the present study together with the data from previous ^{248}Cm(α, t) and ^{248}Cm(^{3}He, d) reactions, the following single-particle states have been identified in ^{249}Bk: 7/2$^+$[633], 0.0 keV; 3/2$^-$[521], 8.78 keV; 1/2$^+$[400], 377.55 keV; 5/2$^+$[642], 389.17 keV; 1/2$^-$[530], 569.20 keV; 1/2$^-$[521], 643.0 keV; 5/2$^-$[523], 672.9 keV; and 9/2$^+$[624], 1075.1 keV. Four vibrational bands were identified at 767.9, 932.2, 1150.7, and 1223.0 keV with tentative assignments of $\{7/2^+$ [633] $\otimes$ 1$^-\}$9/2$^-$, $\{7/2^+$ [633] $\otimes 0^-\}$7/2$^-$, $\{7/2^+$ [633] $\otimes 1^-\}$5/2$^-$, and $\{7/2^+$ [633] $\otimes 0^+\}$7/2$^+$, respectively. A band at 899.9 keV was observed in γ-γ coincidence measurements and given a tentative spin assignment of 3/2. It is possibly associated with a 2$^-$ phonon coupled to the ground state, with configuration $\{7/2^+$ [633] $\otimes 2^-\}$3/2$^-$. Three levels at 624.3, 703.5, and 769.1 keV were assigned spins of 5/2, 7/2, and 9/2, respectively. These could be the members of the 3/2$^+$ [651] band, expected in this energy region.

I. INTRODUCTION

To test theoretical models that predict gaps in the proton single-particle spectra of superheavy nuclei, researchers need experimental energies of single-proton states in the heaviest nuclei. The nuclide ^{253}Es ($t_{1/2} = 20.47$ d) is the heaviest odd-proton nuclide available in millicurie quantities, sufficient for detailed spectroscopy. About 1 mg of this isotope is produced in the High Flux Isotope Reactor (HFIR) at Oak Ridge National Laboratory in each irradiation cycle. However, this Es sample contains $\sim$0.4% ^{254}Es ($t_{1/2} = 275.7$ d) whose daughter ^{250}Bk ($t_{1/2} = 3.217$ h) decays by intense γ rays of 989.13 and 1031.85 keV. These γ rays produce a large Compton background and, thus, reduce the sensitivity of any ^{253}Es measurement. We, therefore, used second-chance Es, which was obtained by milking the ^{253}Es that grew in a ^{253}Cf ($t_{1/2} = 17.81$ d) sample and contained much less ^{254}Es than first-chance Es.

The level structure of ^{249}Bk has previously been studied by measuring the γ rays associated with the α decay of ^{253}Es [1] and β^- decay of ^{249}Cm ($t_{1/2} = 65.3$ min) [1]. The results of these studies have been published in Nuclear Data compilations, but not in any journal. High-resolution α spectra of ^{253}Es were measured by Ahmad and Milsted [2] and by Baranov *et al.* [3], and one-proton transfer reaction experiments were performed on ^{248}Cm targets [4,5]. These studies provide the energies of single-particle orbitals in ^{249}Bk. A level scheme of ^{249}Bk deduced from these studies has been compiled in the Nuclear Data Sheets [1].

Larger germanium detectors and large Compton-suppressed Ge detector arrays have become available, and we have used them to carry out new, more sensitive measurements. Three samples of second-chance ^{253}Es, $\sim$20 mCi each, were obtained from Oak Ridge National Laboratory in 1998, 2000, and 2003. The sample obtained in 1998 was placed in a glass bottle. Its γ-ray spectra contained γ rays from the reactions of intense α particles with light elements (^{14}N, ^{19}F, ^{23}Na, ^{28}Si, and ^{35}Cl). The high-energy γ rays produced in these reactions interfered with weak γ rays of ^{253}Es and also increased the background under the peaks, reducing the sensitivity of the measurement. For this reason, the 2000 and 2003 sources were sandwiched between either two quartz disks for the measurement of low-energy γ rays or two Pt disks for the high-energy spectrum. The source sandwiched between Pt disks was not in contact with any light element or air. This reduced the unwanted γ-ray peaks produced by the reaction of α particles on light elements. The sample produced in 2003 was extremely pure (chemically and isotopically) and provided the most sensitive measurements. It had $\sim$200 times less ^{254}Es than a first-chance Es sample.

II. EXPERIMENTAL METHODS AND RESULTS

A. ^{253}Es α decay

γ-ray singles spectra of the three ^{253}Es samples were measured with two different Ge detectors. The low-energy
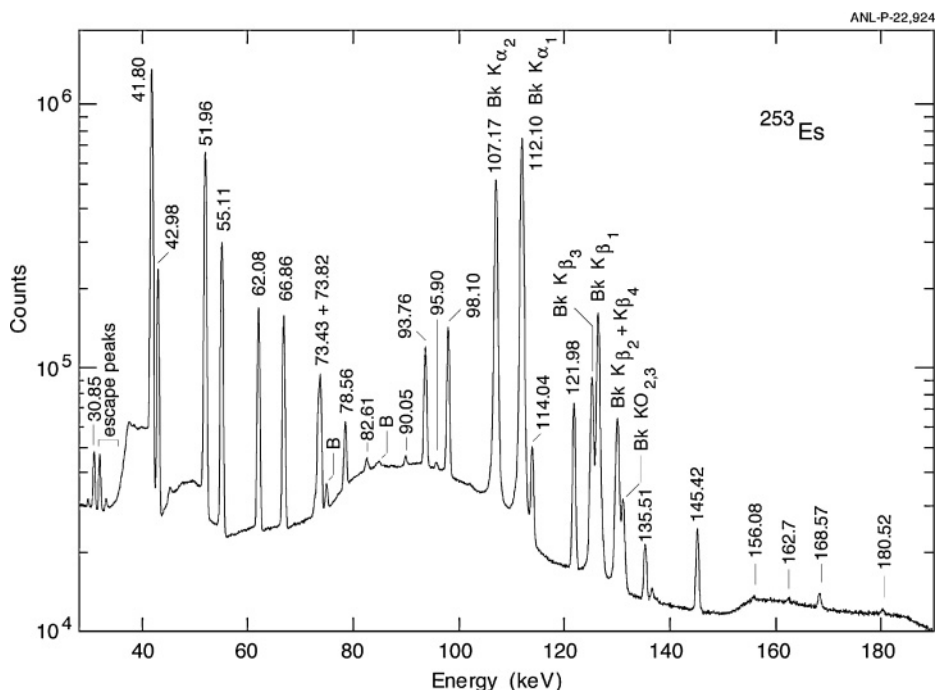
FIG. 1. A ^{253}Es γ-ray spectrum measured with a 5-cm^2×10-mm LEPS spectrometer one week after chemical separation. The sample strength was ~16 mCi, and it was sandwiched between two 1-mm quartz plates. The source-to-detector distance was 18 cm and the counting time was 61 h. A set of Cu and Al absorbers was used to attenuate the Bk L x rays. B denotes Pb K x rays.

γ-ray spectra were measured with a 5-cm^2×10-mm low-energy photon spectrometer (LEPS) and with a 2-cm^2 × 10-mm LEPS detector. The smaller LEPS detector had better resolution and was helpful in resolving close-lying γ lines. Because of better resolution, the LEPS spectra provided more accurate energies for γ rays below 600 keV. The spectra of the 2003 source measured with the LEPS are shown in Figs. 1 and 2. The high-energy portions of the ^{253}Es spectrum were measured with a 25% Ge detector and these are displayed in Fig. 3. The energies of γ rays were measured using internal standards, i.e., the spectra of ^{253}Es and calibration sources were

measured simultaneously. The efficiencies of various detectors were determined with a calibrated mixed source containing ^{109}Cd, ^{57}Co, ^{139}Ce, ^{203}Hg, ^{113}Sn, ^{85}Sr, ^{137}Cs, ^{88}Y, and ^{60}Co. Absolute γ-ray intensities were determined by measuring the α-particle rate of a thin ^{253}Es source with a Si detector of known solid angle and the γ-ray spectrum with a Ge spectrometer whose efficiency was determined with a calibrated source. The γ-ray energies and intensities obtained in the present work are given in Table I. The energy of each level was determined from the most precise energy of a transition deexciting that level.
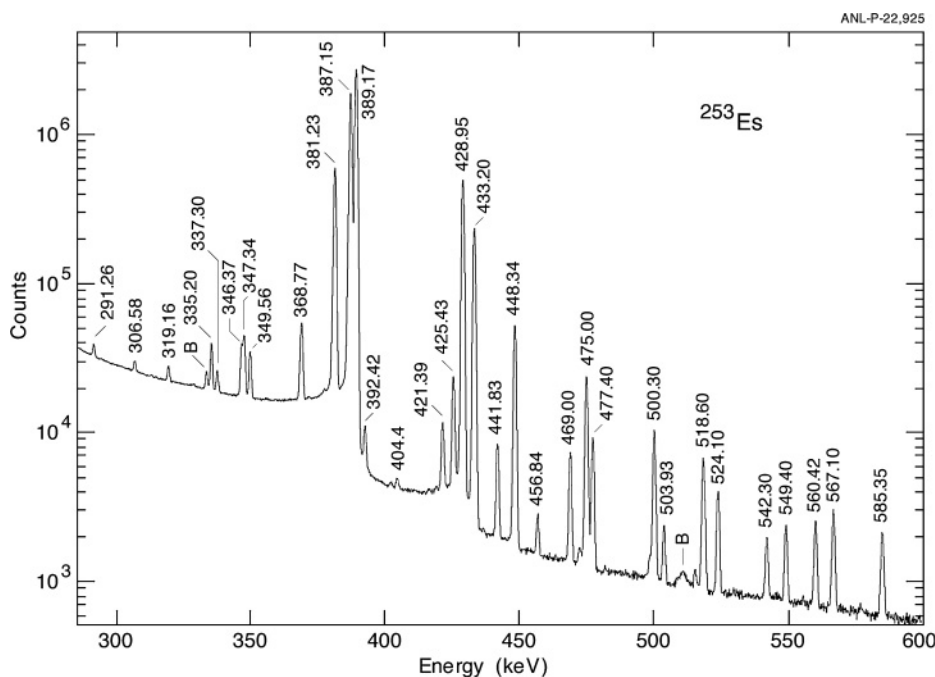

FIG. 2. A ^{253}Es γ-ray spectrum measured with a 5-cm^2×10-mm LEPS detector two weeks after chemical separation. The source was sandwiched between two 0.5-g/cm^2 Pt disks, and it had a strength of ~4 mCi. A set of Ta, Cd, Cu, and Fe absorbers was used to attenuate Bk K x rays and low-energy γ rays. The source-to-detector distance was ~1.0 cm and the counting time was 100 h. B denotes the 333.4-keV γ ray of ^{249}Cf and the 511.0-keV annihilation radiation.
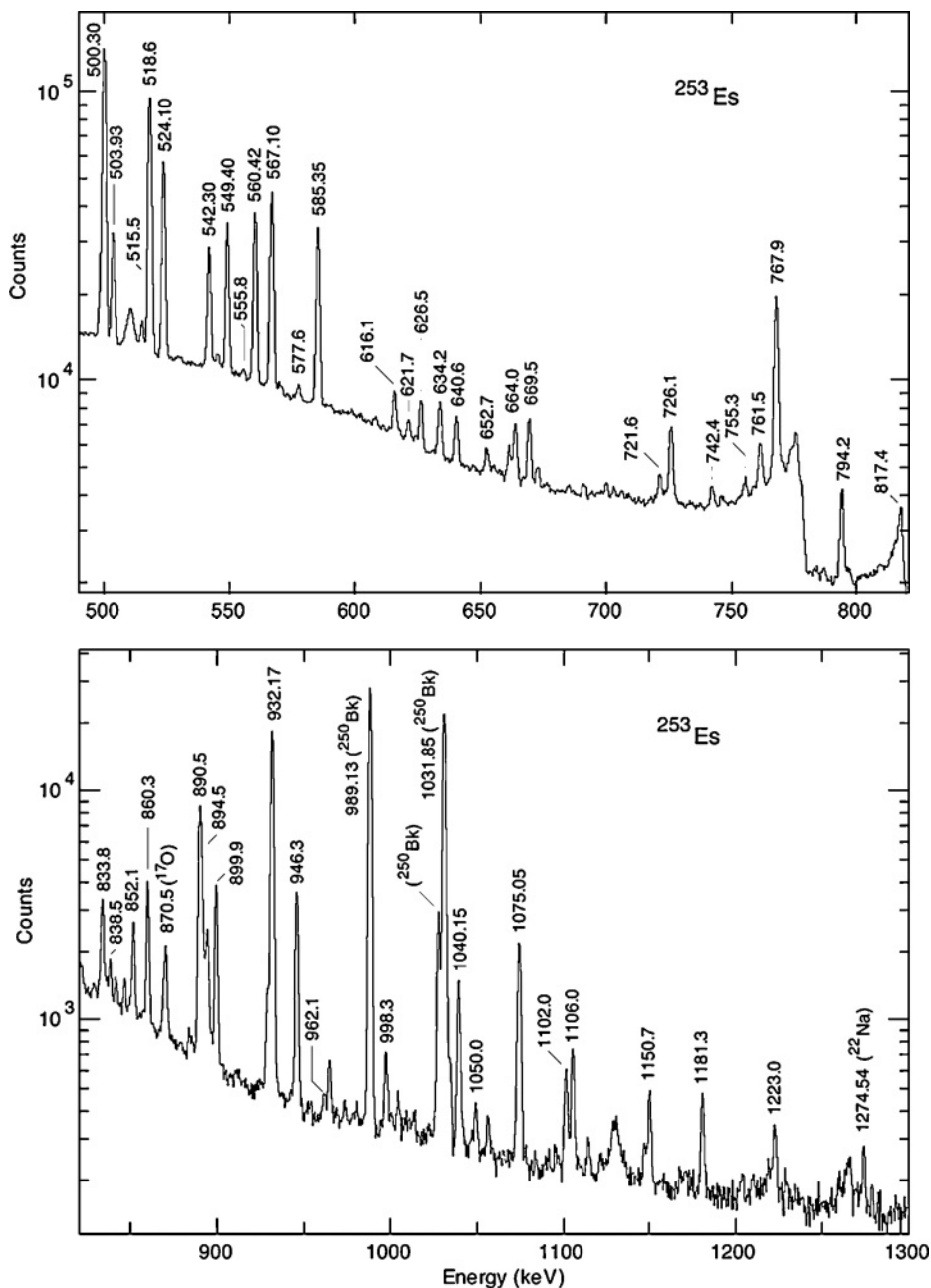
FIG. 3. γ-ray spectrum of a $\sim$4 mCi ^{253}Es source, sandwiched between two 0.5-g/cm^2 Pt disks, measured with a 25% Ge detector through a set of Ta, Cd, Cu, and Fe absorbers, 2 days after chemical purification. The source-to-detector distance was 4.0 cm, and the counting time was 100 h.

γ-ray spectra of ^{253}Es samples were also measured at Livermore in the seventies. The γ-ray energies and intensities measured in that work are compiled in Ref. [1] and agree with the results obtained in the present study. However, because of the isotopically purer source and the enhanced sensitivity of the larger Ge detector, more transitions were identified in this work.

α-γ coincidence measurements were performed to confirm the assignment of γ rays to the ^{253}Es decay. The α particles were detected with a 2.0-cm^2 Si detector and the γ rays with a 110% Ge detector. In the coincidence γ-ray spectrum gated by 4.45–6.20 MeV α particles, strong γ rays seen in the singles spectrum were identified. These include lines with energies 726.1, 767.9, 890.5, 899.9, 932.2, 946.3, 1040.2, and 1075.1 keV. The strong, low-

energy γ rays were observed in a spectrum gated by all ^{253}Es α particles.

To obtain further information on coincidence relationships and to boost the sensitivity for placement of weak γ rays into the ^{249}Bk level scheme, a 6-day long γ-γ coincidence measurement was performed at Argonne National Laboratory. The $\sim$16-mCi source, obtained in 2003, was placed in the center of the GAMMASPHERE spectrometer [6] that comprised 99 Compton-suppressed Ge detectors for this experiment. Although the γ-ray singles spectra, shown in Figs. 1–3, demonstrate that the ^{253}Es sample was extremely pure, the target chamber and materials surrounding the Ge detectors contained radioactivities of ^{48}V, ^{52}Mn, ^{56}Co, ^{56}Ni, ^{58}Co, and ^{96}Tc, produced by nuclear reactions during experiments preceding the present measurement. The data were sorted

TABLE I. ^{253}Es γ rays. Singles spectra were measured with a 5-cm^2 $\times$ 10-mm LEPS detector and a 25% Ge detector. Letter c denotes γ rays seen in γ-γ coincidence measurement only. γ rays not placed in the level scheme are given at the end of the table.

TABLE I. *(Continued.)*

Energy (keV)	Intensity (%)	Transition Initial $\rightarrow$ Final (keV)
30.85 ± 0.01	$(5.5 \pm 0.5) \times 10^{-3}$	$39.63 \rightarrow 8.78$
41.80 ± 0.01	$(5.6 \pm 0.4) \times 10^{-2}$	$41.80 \rightarrow 0.0$
42.98 ± 0.01	$(8.0 \pm 0.8) \times 10^{-3}$	$82.61 \rightarrow 39.63$
51.96 ± 0.01	$(1.38 \pm 0.08) \times 10^{-2}$	$93.76 \rightarrow 41.80$
55.11 ± 0.01	$(5.5 \pm 0.4) \times 10^{-3}$	$137.72 \rightarrow 82.61$
62.08 ± 0.01	$(2.6 \pm 0.2) \times 10^{-3}$	$155.84 \rightarrow 93.76$
66.86 ± 0.01	$(2.1 \pm 0.2) \times 10^{-3}$	$204.58 \rightarrow 137.72$
73.43 ± 0.02	$(5.7 \pm 0.5) \times 10^{-4}$	$229.27 \rightarrow 155.84$
73.82 ± 0.01	$(9.5 \pm 0.9) \times 10^{-4}$	$82.61 \rightarrow 8.78$
78.56 ± 0.01	$(4.1 \pm 0.3) \times 10^{-4}$	$283.14 \rightarrow 204.58$
82.61 ± 0.02	$(5.2 \pm 0.5) \times 10^{-5}$	$311.88 \rightarrow 229.27$
		$+82.61 \rightarrow 0.0$
87.5 ± 0.2^c	$\sim 1 \times 10^{-6}$	$606.71 \rightarrow 519.19$
90.05 ± 0.02	$(3.1 \pm 0.3) \times 10^{-5}$	$373.19 \rightarrow 283.14$
93.76 ± 0.01	$(1.2 \pm 0.1) \times 10^{-3}$	$93.76 \rightarrow 0.0$
95.90 ± 0.02	$(2.7 \pm 0.3) \times 10^{-5}$	$137.72 \rightarrow 41.80$
98.10 ± 0.01	$(1.65 \pm 0.14) \times 10^{-3}$	$137.72 \rightarrow 39.63$
98.2 ± 0.2^c	$\sim 3 \times 10^{-7}$	$704.8 \rightarrow 606.71$
100.5 ± 0.3^c	$\sim 4 \times 10^{-6}$	$473.6 \rightarrow 373.19$
102.8 ± 0.3^c	$\sim 1 \times 10^{-7}$	$709.1 \rightarrow 606.71$
107.17 ± 0.01	$(9.3 \pm 0.3) \times 10^{-3}$	Bk $K\alpha_2$
112.10 ± 0.01	$(1.5 \pm 0.1) \times 10^{-2}$	Bk $K\alpha_1$
114.04 ± 0.01	$(4.7 \pm 0.3) \times 10^{-4}$	$155.84 \rightarrow 41.80$
121.98 ± 0.01	$(1.15 \pm 0.10) \times 10^{-3}$	$204.58 \rightarrow 82.61$
125.42 ± 0.02	$(1.86 \pm 0.15) \times 10^{-3}$	Bk $K\beta_3$
126.57 ± 0.02	$(3.61 \pm 0.2) \times 10^{-3}$	Bk $K\beta_1$
127.36 ± 0.05	$(1.96 \pm 0.2) \times 10^{-4}$	Bk $K\beta_5$
130.24 ± 0.02	$(1.47 \pm 0.12) \times 10^{-3}$	Bk $K\beta_2 + K\beta_4$
131.30 ± 0.02	$(4.5 \pm 0.4) \times 10^{-4}$	Bk $KO_{2,3}$
135.51 ± 0.01	$(1.9 \pm 0.2) \times 10^{-4}$	$229.27 \rightarrow 93.76$
136.81 ± 0.02	$(3.5 \pm 0.3) \times 10^{-5}$	$558.20 \rightarrow 421.39$
137.71 ± 0.05	$(1.0 \pm 0.2) \times 10^{-5}$	$137.72 \rightarrow 0.0$
145.42 ± 0.01	$(3.3 \pm 0.2) \times 10^{-4}$	$283.14 \rightarrow 137.72$
152.2 ± 0.2	$\sim 2 \times 10^{-7}$	$671.3 \rightarrow 519.19$
156.08 ± 0.08	$(1.5 \pm 0.3) \times 10^{-5}$	$311.88 \rightarrow 155.84$
162.7 ± 0.1	$(1.5 \pm 0.4) \times 10^{-5}$	$204.58 \rightarrow 41.80$
164.4 ± 0.3^c	$\sim 3 \times 10^{-7}$	$932.2 \rightarrow 767.9$
168.57 ± 0.08	$(5.3 \pm 0.5) \times 10^{-5}$	$373.19 \rightarrow 204.58$
168.8 ± 0.2^c	$\sim 5 \times 10^{-6}$	$558.20 \rightarrow 389.17$
		$+597.67 \rightarrow 428.95$
180.52 ± 0.08	$(2.1 \pm 0.3) \times 10^{-5}$	$558.20 \rightarrow 377.55$
185.3 ± 0.1	$(8.0 \pm 2.0) \times 10^{-6}$	$606.71 \rightarrow 421.39$
185.6 ± 0.2^c	$\sim 1 \times 10^{-6}$	$704.8 \rightarrow 519.19$
189.4 ± 0.1	$\sim 5 \times 10^{-6}$	$283.14 \rightarrow 93.76$
190.5 ± 0.3	$\sim 5 \times 10^{-6}$	$473.6 \rightarrow 283.14$
191.7 ± 0.2^c	$\sim 7 \times 10^{-7}$	$569.20 \rightarrow 377.55$
192.0 ± 0.2^c	$\sim 6 \times 10^{-7}$	$711.1 \rightarrow 519.19$
203.1 ± 0.5^c	$\sim 3 \times 10^{-7}$	$624.3 \rightarrow 421.39$
		$+624.98 \rightarrow 421.39$
227.0 ± 0.3	$\sim 5 \times 10^{-6}$	$899.9 \rightarrow 672.9$
227.1 ± 0.2^c	$\sim 2 \times 10^{-6}$	$769.1 \rightarrow 542.10$
228.4 ± 0.2^c	$\sim 1 \times 10^{-6}$	$703.5 \rightarrow 475.00$
235.1 ± 0.2^c	$\sim 3 \times 10^{-6}$	$624.3 \rightarrow 389.17$
236.1 ± 0.2^c	$\sim 2 \times 10^{-6}$	$711.1 \rightarrow 475.00$
244.0 ± 0.2^c	$\sim 1 \times 10^{-6}$	$672.9 \rightarrow 428.95$
258.9 ± 0.2^c	$\sim 2 \times 10^{-6}$	$542.10 \rightarrow 283.14$
261.7 ± 0.3^c	$\sim 8 \times 10^{-7}$	$934.7 \rightarrow 672.9$
270.46 ± 0.08	$(1.8 \pm 0.2) \times 10^{-5}$	$475.00 \rightarrow 204.58$
274.5 ± 0.2^c	$\sim 1 \times 10^{-6}$	$703.5 \rightarrow 428.95$
282.2 ± 0.2^c	$\sim 1 \times 10^{-6}$	$711.1 \rightarrow 428.95$
283.7 ± 0.2	$\sim 5 \times 10^{-6}$	$672.9 \rightarrow 389.17$
		$+661.3 \rightarrow 377.55$
291.26 ± 0.08	$(3.4 \pm 0.3) \times 10^{-5}$	$428.95 \rightarrow 137.72$
294.1 ± 0.2^c	$\sim 1 \times 10^{-6}$	$769.1 \rightarrow 475.00$
306.58 ± 0.08	$(2.4 \pm 0.2) \times 10^{-5}$	$389.17 \rightarrow 82.61$
312.7 ± 0.1	$(4.5 \pm 0.6) \times 10^{-6}$	$542.10 \rightarrow 229.27$
314.2 ± 0.2^c	$\sim 2 \times 10^{-6}$	$703.5 \rightarrow 389.17$
319.16 ± 0.05	$(3.7 \pm 0.3) \times 10^{-5}$	$475.00 \rightarrow 155.84$
335.20 ± 0.05	$(1.40 \pm 0.15) \times 10^{-4}$	$428.95 \rightarrow 93.76$
337.30 ± 0.05	$(5.2 \pm 0.4) \times 10^{-5}$	$475.00 \rightarrow 137.72$
340.2 ± 0.5	$\sim 5 \times 10^{-7}$	$769.1 \rightarrow 428.95$
346.37 ± 0.05	$(1.6 \pm 0.2) \times 10^{-4}$	$428.95 \rightarrow 82.61$
347.34 ± 0.05	$(2.0 \pm 0.3) \times 10^{-4}$	$389.17 \rightarrow 41.80$
349.56 ± 0.05	$(1.4 \pm 0.2) \times 10^{-4}$	$389.17 \rightarrow 39.63$
368.77 ± 0.02	$(3.6 \pm 0.2) \times 10^{-4}$	$377.55 \rightarrow 8.78$
		$+597.67 \rightarrow 229.27$
381.23 ± 0.02	$(5.5 \pm 0.3) \times 10^{-3}$	$475.00 \rightarrow 93.76$
387.15 ± 0.02	$(1.90 \pm 0.10) \times 10^{-2}$	$428.95 \rightarrow 41.80$
389.17 ± 0.02	$(2.70 \pm 0.10) \times 10^{-2}$	$389.17 \rightarrow 0.0$
392.42 ± 0.05	$(4.4 \pm 0.4) \times 10^{-5}$	$475.00 \rightarrow 82.61$
402.0 ± 0.1	$(5.0 \pm 1.0) \times 10^{-6}$	$410.6 \rightarrow 8.78$
		$+606.71 \rightarrow 204.58$
404.4 ± 0.1	$(8.0 \pm 0.8) \times 10^{-6}$	$542.10 \rightarrow 137.72$
416.3 ± 0.2	$(1.4 \pm 0.3) \times 10^{-6}$	$498.6 \rightarrow 82.61$
421.39 ± 0.03	$(8.5 \pm 0.4) \times 10^{-5}$	$421.39 \rightarrow 0.0$
421.7 ± 0.2^c	$\sim 8 \times 10^{-6}$	$704.8 \rightarrow 283.14$
425.43 ± 0.02	$(2.22 \pm 0.15) \times 10^{-4}$	$519.19 \rightarrow 93.76$
428.95 ± 0.02	$(5.55 \pm 0.20) \times 10^{-3}$	$428.95 \rightarrow 0.0$
433.20 ± 0.02	$(2.7 \pm 0.2) \times 10^{-3}$	$475.00 \rightarrow 41.80$
436.8 ± 0.4	$\sim 1.0 \times 10^{-6}$	$519.19 \rightarrow 82.61$
441.83 ± 0.02	$(7.9 \pm 0.8) \times 10^{-5}$	$597.67 \rightarrow 155.84$
		$+671.3 \rightarrow 229.27$
448.34 ± 0.02	$(6.4 \pm 0.3) \times 10^{-4}$	$542.10 \rightarrow 93.76$
456.84 ± 0.08	$(1.6 \pm 0.2) \times 10^{-5}$	$498.6 \rightarrow 41.80$
469.00 ± 0.05	$(8.0 \pm 0.7) \times 10^{-5}$	$606.71 \rightarrow 137.72$
472.6 ± 0.2	$(4 \pm 1) \times 10^{-6}$	$701.9 \rightarrow 229.27$
475.00 ± 0.05	$(3.2 \pm 0.2) \times 10^{-4}$	$475.00 \rightarrow 0.0$
477.40 ± 0.05	$(1.12 \pm 0.10) \times 10^{-4}$	$519.19 \rightarrow 41.80$
498.6 ± 0.2	$(5.7 \pm 0.6) \times 10^{-6}$	$498.6 \rightarrow 0.0$
500.30 ± 0.05	$(1.43 \pm 0.12) \times 10^{-4}$	$542.10 \rightarrow 41.80$
		$+704.8 \rightarrow 204.58$
503.93 ± 0.05	$(2.1 \pm 0.2) \times 10^{-5}$	$597.67 \rightarrow 93.76$
515.5 ± 0.1	$(3.5 \pm 0.6) \times 10^{-6}$	$671.3 \rightarrow 155.84$
518.60 ± 0.08	$(1.02 \pm 0.10) \times 10^{-4}$	$558.20 \rightarrow 39.63$
		$+723.2 \rightarrow 204.58$
524.10 ± 0.05	$(5.2 \pm 0.5) \times 10^{-5}$	$606.71 \rightarrow 82.61$
530.0 ± 0.3	$\sim 1.0 \times 10^{-6}$	$569.20 \rightarrow 39.63$
542.30 ± 0.05	$(2.2 \pm 0.2) \times 10^{-5}$	$624.98 \rightarrow 82.61$
545.9 ± 0.3	$(1.5 \pm 0.3) \times 10^{-6}$	$701.9 \rightarrow 155.84$

TABLE I. *(Continued.)*

Energy (keV)	Intensity (%)	Transition Initial → Final (keV)
549.40 ± 0.05	$(3.0 \pm 0.2) \times 10^{-5}$	558.20 → 8.78
555.8 ± 0.3	$(1.2 \pm 0.3) \times 10^{-6}$	597.67 → 41.80
560.42 ± 0.05	$(3.5 \pm 0.3) \times 10^{-5}$	569.20 → 8.78
567.10 ± 0.05	$(4.5 \pm 0.3) \times 10^{-5}$	606.71 → 39.63
		+704.8 → 137.72
571.0 ± 0.3	$\sim 1.0 \times 10^{-6}$	709.1 → 137.72
577.6 ± 0.2	$(1.5 \pm 0.2) \times 10^{-6}$	671.3 → 93.76
585.35 ± 0.05	$(3.4 \pm 0.2) \times 10^{-5}$	624.98 → 39.63
590.1 ± 0.3^c	$\sim 1.0 \times 10^{-6}$	672.9 → 82.61
608.2 ± 0.3	$\sim 5 \times 10^{-7}$	701.9 → 93.76
616.1 ± 0.2	$(3.6 \pm 0.3) \times 10^{-6}$	624.98 → 8.78
621.7 ± 0.2	$(1.8 \pm 0.2) \times 10^{-6}$	661.3 → 39.63
624.3 ± 0.4	$(7 \pm 2) \times 10^{-7}$	624.3 → 0.0
626.5 ± 0.2	$(4.0 \pm 0.3) \times 10^{-6}$	709.1 → 82.61
633.0 ± 0.3^c	$\sim 2.0 \times 10^{-6}$	672.9 → 39.63
634.2 ± 0.2	$(4.7 \pm 0.4) \times 10^{-6}$	643.0 → 8.78
640.6 ± 0.2	$(3.4 \pm 0.3) \times 10^{-6}$	723.2 → 82.61
652.7 ± 0.2	$(1.20 \pm 0.15) \times 10^{-6}$	661.3 → 8.78
661.6 ± 0.2	$(2.4 \pm 0.4) \times 10^{-6}$	703.5 → 41.80
664.0 ± 0.2	$(5.0 \pm 0.5) \times 10^{-6}$	672.9 → 8.78
669.5 ± 0.2	$(5.8 \pm 0.5) \times 10^{-6}$	709.1 → 39.63
672.8 ± 0.2	$(1.4 \pm 0.3) \times 10^{-6}$	672.9 → 0.0
700.3 ± 0.3	$(4 \pm 1) \times 10^{-7}$	709.1 → 8.78
703.6 ± 0.4	$\sim 2 \times 10^{-7}$	703.5 → 0.0
721.6 ± 0.2	$(1.5 \pm 0.2) \times 10^{-6}$	1150.7 → 428.95
726.1 ± 0.2	$(5.4 \pm 0.4) \times 10^{-6}$	767.9 → 41.80
742.4 ± 0.3	$(8.5 \pm 1.0) \times 10^{-7}$	836.1 → 93.76
755.3 ± 0.3	$(1.2 \pm 0.2) \times 10^{-6}$	911.2 → 155.84
761.5 ± 0.2	$(3.1 \pm 0.3) \times 10^{-6}$	1150.7 → 389.17
767.9 ± 0.1	$(3.1 \pm 0.2) \times 10^{-5}$	767.9 → 0.0
794.0 ± 0.2^c	$(1.5 \pm 0.2) \times 10^{-6}$	1223.0 → 429.0
794.2 ± 0.2	$(2.6 \pm 0.3) \times 10^{-6}$	836.1 → 41.80
817.4 ± 0.3	$(5.0 \pm 0.5) \times 10^{-6}$	911.2 → 93.76
833.8 ± 0.2	$(4.7 \pm 0.4) \times 10^{-6}$	1223.0 → 389.17
836.1 ± 0.2	$(6.2 \pm 0.8) \times 10^{-7}$	836.1 → 0.0
838.5 ± 0.3	$(1.2 \pm 0.2) \times 10^{-6}$	932.2 → 93.76
852.1 ± 0.2	$(3.1 \pm 0.2) \times 10^{-6}$	934.7 → 82.61
860.3 ± 0.2	$(6.0 \pm 0.4) \times 10^{-6}$	899.9 → 39.63
890.5 ± 0.2	$(2.2 \pm 0.2) \times 10^{-5}$	932.2 → 41.80
		+899.9 → 8.78
894.5 ± 0.2	$(5.2 \pm 0.5) \times 10^{-6}$	988.1 → 93.76
899.9 ± 0.1	$(7.2 \pm 0.5) \times 10^{-6}$	1055.8 → 155.84
932.17 ± 0.05	$(4.1 \pm 0.2) \times 10^{-5}$	932.2 → 0.0
946.3 ± 0.1	$(7.8 \pm 0.5) \times 10^{-6}$	988.1 → 41.80
962.1 ± 0.1	$(2.4 \pm 0.4) \times 10^{-7}$	1055.8 → 93.76
981.3 ± 0.3	$\sim 1.0 \times 10^{-7}$	1075.1 → 93.76
998.3 ± 0.1	$(9.0 \pm 0.9) \times 10^{-7}$	1227.6 → 229.27
1014.4 ± 0.5	$\sim 2 \times 10^{-7}$	1055.8 → 41.80
∼1033	$\sim 1.0 \times 10^{-6}$	1075.1 → 41.8
1040.15 ± 0.08	$(3.0 \pm 0.2) \times 10^{-6}$	1133.9 → 93.76
1050.0 ± 0.2	$(4.2 \pm 0.5) \times 10^{-7}$	1143.8 → 93.76
1075.05 ± 0.08	$(5.8 \pm 0.4) \times 10^{-6}$	1075.1 → 0.0
1102.0 ± 0.2	$(1.4 \pm 0.2) \times 10^{-6}$	1143.8 → 41.80
1150.7 ± 0.2	$(8.0 \pm 0.8) \times 10^{-7}$	1150.7 → 0.0
1181.3 ± 0.2	$(1.0 \pm 0.1) \times 10^{-6}$	1223.0 → 41.8
1223.0 ± 0.2	$(6.0 \pm 0.6) \times 10^{-7}$	1223.0 → 0.0

TABLE I. *(Continued.)*

Energy (keV)	Intensity (%)	Transition Initial → Final (keV)
482.1 ± 0.5	$\sim 1.0 \times 10^{-6}$	unassigned
842.0 ± 0.3	$(9 \pm 2) \times 10^{-7}$	unassigned
847.0 ± 0.3	$(6 \pm 1) \times 10^{-7}$	unassigned
965.2 ± 0.3	$(8 \pm 2) \times 10^{-7}$	unassigned
1005.3 ± 0.5	$\sim 4 \times 10^{-7}$	unassigned
1023.0 ± 0.5	$\sim 1.0 \times 10^{-7}$	unassigned
1034.7 ± 0.5	$\sim 1.0 \times 10^{-6}$	unassigned
1042.3 ± 0.5	$\sim 1.7 \times 10^{-7}$	unassigned
1057.1 ± 0.5	$(3.8 \pm 0.6) \times 10^{-7}$	unassigned
1106.0 ± 0.2	$(1.8 \pm 0.2) \times 10^{-6}$	unassigned

offline into two-dimensional γ-γ coincidence matrices, and γ-ray spectra were generated by placing gates on various γ-ray peaks. The gated spectra contained three kinds of peaks: true coincidences between photopeaks, random coincidences, and Compton-Compton peaks. The 2-keV-wide coincidence gate contained the full energy events from the γ ray of interest and Compton events from higher energy γ rays. Compton-scattered photons which entered a second detector had a unique energy: a strong γ ray with energy E_γ will generate Compton peaks in two detectors with energies E_1 and E_2 such that $E_1 + E_2 = E_\gamma$. Since the singles spectrum was well determined in the previous measurements, it was easy to identify random peaks as well as Compton scattered peaks. To ensure that two γ rays were in coincidence with each other, spectra generated by placing a gate on each γ-ray peak were examined. We also compared γ-ray spectra gated by several γ rays deexciting the same level or feeding the same level to ascertain that the γ rays belonged to ^{253}Es decay. The sensitivity of GAMMASPHERE was sufficient to identify γ rays with intensity as low as 1.0×10^{-6}% per ^{253}Es α decay in the gated spectra, but because of intense Compton peaks, it was not possible, in some instances, to identify weak γ lines.

The results from the analysis of these data are given in Table II and an example of a coincidence spectrum is shown in Fig. 4. For low-energy γ rays, the Bk K x-ray yield was used to deduce transition multipolarities. In several cases, some weak γ rays were expected to be in coincidence with a gate, but these were not observed in the gated spectrum due to low statistics. We have not included such γ rays in the table. γ rays observed in coincidence with a gate but not placed in the ^{249}Bk level scheme are denoted by an asterisk in the Table II. Since these γ rays do not fit in a coherent level scheme, it is not clear whether they belong to the decay of ^{253}Es. Energies of weak γ rays were determined with respect to energies of stronger γ rays measured in the γ-singles spectra and have uncertainties of less than 0.2 keV. Only approximate intensities were obtained from the coincidence data.

γ-γ coincidence measurements were also carried out at Livermore using two Ge(Li) detectors. This experiment was more sensitive to low-energy γ rays, and the coincidence information obtained from this measurement is included in Table II. The dispersion of the γ-ray spectra was 1.6 keV/channel, and hence the energies of the weak γ rays

TABLE II. Results of ^{253}Es γ-γ coincidence measurements with GAMMASPHERE. Asterisk denotes γ ray was not placed in level scheme. Transitions shown in parenthesis are not listed in Table I.

Gate γ-ray Energy (keV)	Gate transition Initial → Final (keV)	Energies of γ rays observed (keV)
107.2+112.1	(Kα)	168.8, 227.0, 244.0, 235.1, 283.7, 294.1, 661.6, 664.0, 672.8, 721.6, 726.1, 761.5, 767.9, 794.0, 833.8
122.0	204.58 → 82.61	73.8, 78.6, 168.6, 190.5, 500.3, 518.6
136.8	558.16 → 421.39	368.8, 402.0, 421.4 , 264.7*
145.4	283.14 → 137.72	55.1, 90.1, 98.1, 190.5, 258.9, 421.7
164.4	932.2 → 767.9	726.1, 767.9
168.6	373.19 → 204.58	66.9, 100.5, 122.0
185.3	606.71 → 421.39	368.8, 402.0, 421.4
227.0	899.9 → 672.9	244.0, 283.7, 590.1, 633.0, 664.0, 672.8
	769.1 → 542.1	448.3, 500.3
283.7	672.8 → 389.17	227.0, 261.7, 389.2
368.8	377.55 → 8.78	136.8, 180.5, 185.3, 191.7, 203.1, 231.7 (643.0-410.6), 264.1 (643.0-377.6), 283.7, 300.3 (709.1-410.6), 330.7 (709.1-377.6)
	597.67 → 229.27	73.4
389.2	389.17 → 0.0	168.8, 235.1, 283.7, 314.2, 761.5, 833.8
421.4	421.39 → 0.0	136.8, 185.3, 203.1,
421.7	704.8 → 283.1	78.6, 145.4
425.4	519.19 → 93.76	78.8 (597.7-519.2), 87.5, 93.8,134.9 (654.1-519.2), 152.2, 185.6, 192.0, 202.1 (723.2-519.2)
429.0	428.95 → 0.0	54.2 (597.7-542.1), 70.0 (498.6-429.0), 89.9 (519.2-429.0), 122.1 (597.7-475.0), 177.6 (606.7-429.0), 229.0, 244.0, 247.7 (723.2-475.0), 274.5, 282.2, 340.2, 721.6, 794.0
433.2	475.0 → 41.80	228.4, 236.1, 294.1, 748.0 (1223.0-475.0)
441.8	597.67 → 155.84	62.1, 114.0
	671.3 → 229.27	73.4, 135.5
448.3	542.10 → 93.76	93.8, 227.1
469.0	606.71 → 137.72	55.1, 98.2, 102.8
518.6	723.4 → 204.58	66.9, 122.0
524.1	606.71 → 82.61	73.8, 98.2
664.0	672.8 → 8.78	227.0, 261.7
767.9	767.9 → 0.0	Bk x rays, 164.4, 455.1 (1223.0-767.9)

have uncertainties of 1.0 keV. Several weak γ rays, identified in the coincidence spectra, have been placed in the level scheme but are not included in Table I. Their intensities are less than $1 \times 10^{-6}\%$ per decay, and in Table II their placement is shown in parentheses. Table II contains only the highest energy transition of the ground-state and the $3/2^-[521]$ bands in coincidence with a gate; the subsequent transitions in these bands are not listed.

B. ^{249}Cm β^- decay

Information on ^{249}Bk levels was also obtained from β^- decay studies of ^{249}Cm ($t_{1/2} = 65.3$ min). Samples containing ^{249}Cm were prepared via neutron capture reactions on ^{248}Cm targets irradiated[1] in flux levels of $(0.9–1.3) \times 10^{14}$ n/cm^2-sec. The target material was comprised predominantly[2] of ^{248}Cm. A 3-h irradiation of a typical 100-μg ^{248}Cm

sample at the highest neutron flux produced 8×10^7 Bq activity of ^{249}Cm at the end of irradiation. In the last experiment of the series of irradiations, a 1.8-mg ^{248}Cm target was irradiated to near saturation with production of 1.7×10^9 Bq ^{249}Cm activity.

Following irradiation, curium in the target was chemically purified to remove fission products (FP). After dissolution of the target, fluoride and hydroxide coprecipitations with a lanthanum carrier were performed. Most of the remaining FPs and the lanthanum carrier were then removed by elution with HCl ethanol from a column of Dowex 50×12 colloidal cation resin. The procedure required 90–120 min and provided sufficient purification to permit the measurement and identification of ^{249}Cm γ rays over three half-lives with no significant FP interference. Because ^{248}Cm has a significant spontaneous-fission (SF) decay branch (8.39%), FP activities grow into a freshly purified sample relatively rapidly.

The purified curium fraction was analyzed for β^- decay and showed the presence of 65-min ^{249}Cm, 3.22-h ^{250}Bk, and a longer-lived component. The ^{250}Bk/^{249}Cm β^- activity ratio, extrapolated back to the end of the irradiation, was in the range $(0.2–3.0) \times 10^{-3}$, depending upon neutron-flux levels and degrees of chemical separation. The activity ratio of the

---

[1]Irradiations were performed at both the Livermore pool-type reactor and the General Electric test reactor, Vallecitos, CA.

[2]The curium isotopic composition: 97.63% 248, 0.0092% 247, 2.35% 246, 0.011% 245, and 0.0007% 244.
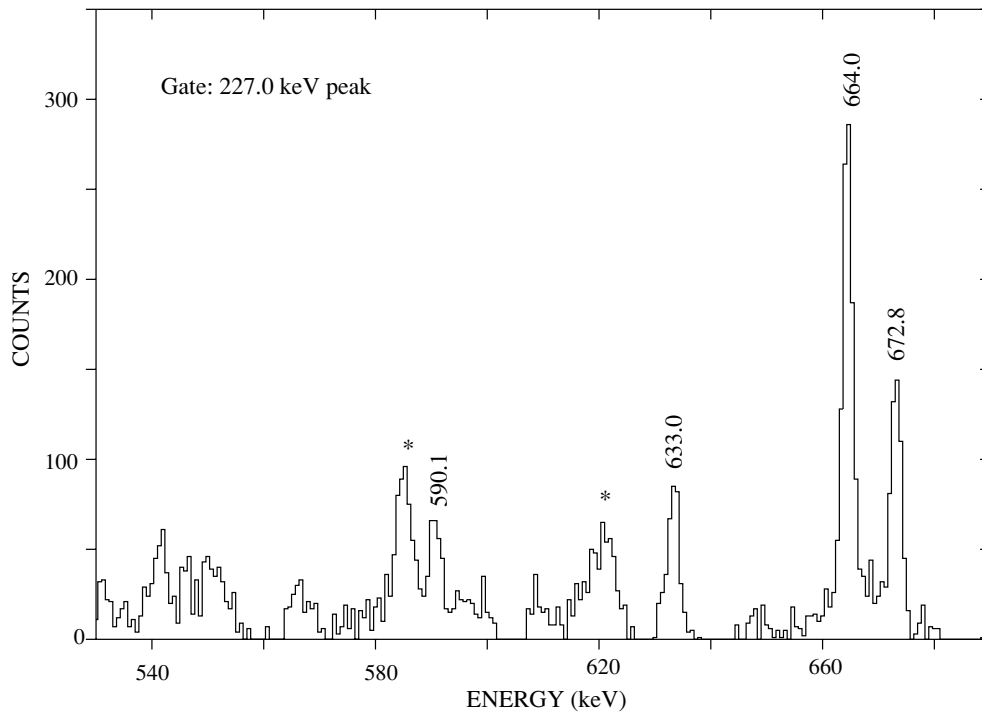
FIG. 4. γ-ray spectrum measured with GAMMASPHERE in coincidence with the 227.0-keV γ ray. γ rays with energies 672.8, 664.0, 633.0, and 590.1 keV are in coincidence with the 227.0-keV γ ray. The spectrum was obtained by subtracting a spectrum gated on background counts from the spectrum gated on the 227.0-keV peak. The stars denote Compton-scattered γ rays. Source strength was $\sim$16 mCi.

long-lived component to ^{249}Cm, also extrapolated back, was $(0.5–1.5) \times 10^{-4}$.

The γ-ray singles spectrum of ^{249}Cm was measured with several Ge(Li) detectors, an 8-cm^3 cylindrical detector, a windowless detector with a 1-cm depletion depth, and a 7-cm^3 rectangular detector. The last detector was equipped with a Compton-suppression shield consisting of a large cylindrical NaI crystal surrounding it. The Ge(Li) detectors were calibrated for geometry and efficiency with standard sources. γ-ray energies were determined with respect to ^{57}Co (122.061 keV), ^{137}Cs (661.660 keV), and ^{54}Mn (834.843 keV) lines by measuring their spectra concurrently with ^{249}Cm samples. The spectra obtained were analyzed with the GAMANAL code [7]. A ^{249}Cm γ-ray spectrum measured with the 8-cm^3 Ge(Li) detector is displayed in Fig. 5 and the γ-ray energies and intensities are listed in Table III. All of the γ rays listed in the table exhibited decay consistent with the 65.3-min half-life of ^{249}Cm. To obtain the absolute intensities listed in the table, a gas-flow proportional counter, serving as a β^- detector, was used. It was calibrated for geometry and efficiency with a ^{198}Au standard whose absolute β^- disintegration rate was determined by counting the 100% abundant 411.8-keV γ ray.

Of the 18 γ rays listed in Table III, 13 have also been observed in the α decay of ^{253}Es. In addition to the γ lines listed in Table III, the more abundant lines from ^{250}Bk decay in the 890–1032 keV range were observed. The 989.1-keV line of ^{250}Bk was identified in each spectrum with the assignment to ^{250}Bk based on the decay with a 3.22-h half-life, a wide

variation in its intensity relative to the lines of ^{249}Cm, and the detection of companion γ rays from ^{250}Bk decay. The presence of small amounts of ^{250}Bk did not provide any significant interference in ^{249}Cm measurements.

A cooled Si(Li) detector was used to measure the spectrum of β^- particles and conversion electrons from ^{249}Cm decay. The end point of the ^{249}Cm β^- spectrum was determined in a Fermi plot, with a calibration provided by ^{250}Bk K conversion lines at 854.2 and 896.9 keV. The value measured for the ^{249}Cm endpoint is 876 ± 15 keV.

C. ^{253}Es fission branch

In the ^{253}Es γ-ray spectrum measured two days after chemical purification and displayed in Fig. 6, we observed 1313.0- and 1435.8-keV γ rays arising from the decay of fission fragments ^{136}I ($t_{1/2} = 45$ s) and ^{138}Cs ($t_{1/2} = 32.2$ min). In a γ-ray spectrum measured 49 days after the isolation of ^{253}Es, the 1596.5-keV γ ray of ^{140}Ba-La ($t_{1/2} = 12.746$ d) was observed. These three γ rays were also seen [8] in the fission of a ^{252}Cf sample. We followed the decay of these γ rays and found that they belonged to the decay of ^{253}Es. We did not detect any longer-lived ^{252}Cf in the ^{253}Es sample. Using the measured intensity of $(3.6 \pm 0.4) \times 10^{-7}\%$ per ^{253}Es α decay for the 1435.8-keV γ ray and 4.49% [9] cumulative yield of ^{138}Cs in ^{253}Es fission, we determine the fission branch of ^{253}Es as $(1.0 \pm 0.1) \times 10^{-5}\%$, which agrees with the literature value [10] of $(8.7 \pm 0.3) \times 10^{-6}\%$.
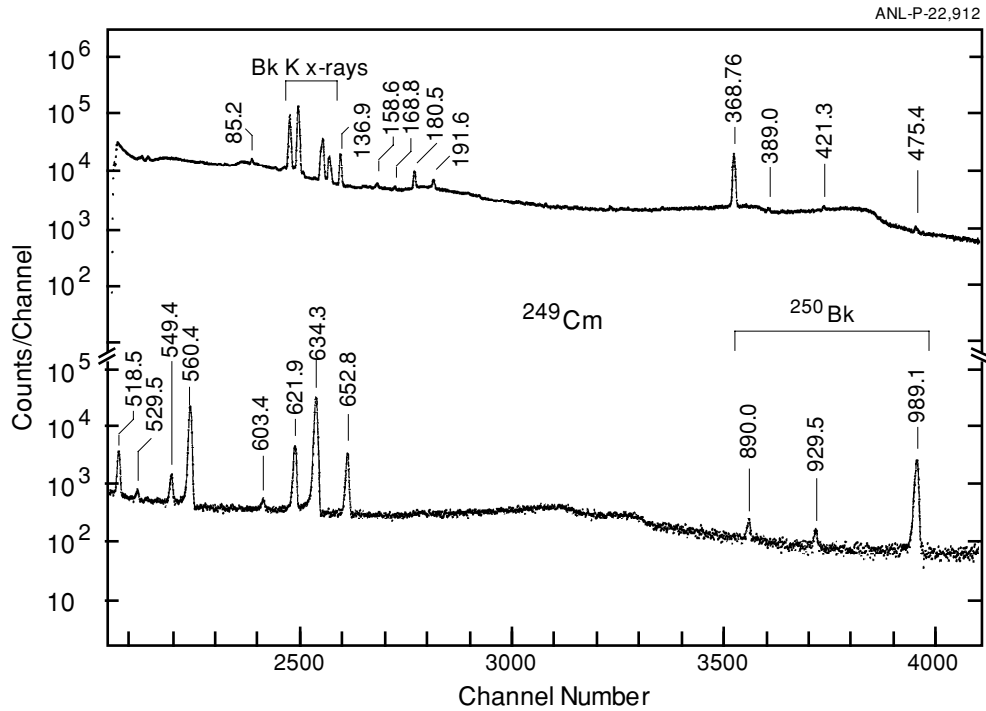
FIG. 5. γ-ray spectrum of a ^{249}Cm source measured with an 8-cm^3 Ge(Li) detector. The break on the *y* axis shows the change in the scale.

III. DISCUSSION

A. Level scheme

Some of the single-particle states in ^{249}Bk, shown in Fig. 7, have been assigned in previous studies. Energies of most of the levels below 700 keV were directly obtained from high-resolution α-particle spectra [2]. In this section, we present the evidence for spin-parity assignments. As discussed later, the spins and parities of low-lying levels are well established from measured transition multipolarities [1]. The spins of high-lying levels can be deduced from the deexcitation patterns of these levels to the members of lower rotational bands. However, the parities of these levels cannot be determined from the experimental data. For parities, we have used α-decay hindrance factors and configurations available for assignments.

The ground-state spin of ^{249}Bk has been measured [11] to be 7/2. The measured magnetic moment [11] of the ^{249}Bk ground state agrees with the value calculated for the 7/2$^+$[633] configuration [12] . Its rotational members up to $I = 17/2$ were identified in the α-singles spectrum [2], and in the present work, we observed the γ rays deexciting these levels. Measured transition multipolarities [1] and coincidence relationships among intraband transitions observed in the present work clearly support the spin-parity assignments.

The level at 8.78 keV was observed in the α-singles spectrum [2,3], and its half-life was determined to be 0.3 ms [1]. This level is strongly populated in the β^- decay of ^{249}Cm suggesting spin 1/2 or 3/2. Measured multipolarities [1] plus measured energies of its rotational members fix the spin-parity of the bandhead as 3/2$^-$. Rotational members with spin up to 17/2 have been identified.

The state at 389.17 keV decays to the ground-state band and also to the 3/2$^-$ band, and the multipolarity of the 389.17-keV transition has been measured [1] to be $M1$. These data fix the spin-parity of the 389.17-keV level as 5/2$^+$. Rotational members up to spin 15/2 have been identified in the present work. The level scheme of ^{249}Bk deduced from the results of the present study is presented in Figs. 7–10.
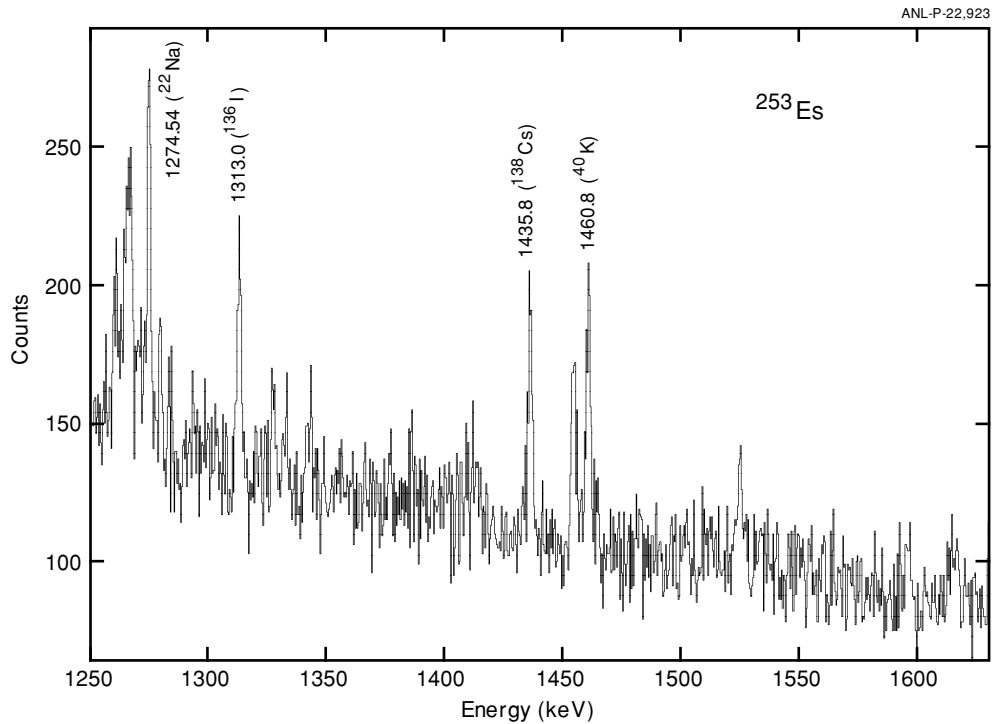
TABLE III. ^{249}Cm γ rays measured with an 8-cm^3 Ge(Li) detector.

Energy (keV)	Intensity (%)	Transitions Initial → Final (keV)
85.2 ± 0.2	$(5.4 \pm 0.5) \times 10^{-3}$	$643.0 \rightarrow 558.2$
136.9 ± 0.1	$(3.9 \pm 0.3) \times 10^{-2}$	$558.2 \rightarrow 421.3$
158.6 ± 0.1	$(2.9 \pm 0.4) \times 10^{-3}$	$569.2 \rightarrow 410.6$
168.8 ± 0.2	$(2.2 \pm 0.2) \times 10^{-3}$	$558.2 \rightarrow 389.2$
180.5 ± 0.1	$(2.0 \pm 0.14) \times 10^{-2}$	$558.2 \rightarrow 377.6$
191.6 ± 0.1	$(1.0 \pm 0.09) \times 10^{-2}$	$569.2 \rightarrow 377.6$
368.76 ± 0.06	0.35 ± 0.023	$377.6 \rightarrow 8.78$
389.0 ± 0.2	$(6.3 \pm 0.8) \times 10^{-3}$	$389.2 \rightarrow 0.0$
421.3 ± 0.2	$(9.2 \pm 1.0) \times 10^{-3}$	$421.3 \rightarrow 0.0$
475.4 ± 0.2	$(7.2 \pm 1.2) \times 10^{-3}$	$558.2 \rightarrow 82.61$
518.5 ± 0.1	$(8.8 \pm 0.6) \times 10^{-2}$	$558.2 \rightarrow 39.63$
529.5 ± 0.2	$(7.0 \pm 0.8) \times 10^{-3}$	$569.2 \rightarrow 39.63$
549.4 ± 0.1	$(3.0 \pm 0.5) \times 10^{-2}$	$558.2 \rightarrow 8.78$
560.4 ± 0.1	0.84 ± 0.06	$569.2 \rightarrow 8.78$
603.4 ± 0.2	$(6.4 \pm 0.9) \times 10^{-3}$	$643.0 \rightarrow 39.63$
621.9 ± 0.1	0.18 ± 0.013	$661.5 \rightarrow 39.63$
634.3 ± 0.1	1.5 ± 0.1	$643.0 \rightarrow 8.78$
652.8 ± 0.1	0.14 ± 0.01	$661.5 \rightarrow 8.78$

FIG. 6. γ-ray spectrum of a ^{253}Es source measured with a 25% Ge detector showing the fission γ rays. This is the high-energy portion of the spectrum shown in Fig. 3. The 1274.54-keV γ ray belongs to the ^{22}Na impurity in the sample and the 1460.8-keV γ ray is due to ^{40}K background.

The ground state of ^{249}Cm has been assigned to the $1/2^+$[620] Nilsson state [13] from the neutron-capture studies [14] and the ^{248}Cm(d, p) reaction cross sections [15]. In ^{249}Bk, the only levels expected to receive measurable β^- population are those with spin 1/2 and 3/2 because $\Delta I = 0$ or 1 transitions are strongly favored. These low spin levels are easily identified in an analysis of the ^{249}Cm γ-ray spectrum. States populated in the decay of ^{249}Cm are displayed in Fig. 10. The level at 377.55 keV decays only to the $3/2^-$ level at 8.78 keV, suggesting $1/2^+$ quantum numbers. γ-γ coincidence data show that the 368.8-, 402.0-, and 421.4-keV γ rays are in coincidence with the 136.8 (558.20-421.39) keV γ ray. This indicates intraband transitions between 421.39-, 410.6-, and 377.55-keV levels and hence these three levels belong to a single rotational band. The decay pattern indicates spins 3/2 and 5/2 for the 410.6- and 421.39-keV levels, respectively. The 7/2, 9/2, and 13/2 members have been identified at 498.6, 519.19, and 671.3 keV. It is observed that states with spin 5/2 and higher decay predominantly to the ground-state $7/2^+$ band, supporting further the positive-parity assignment of this band. From the level energies, we determine the rotational constant of $\hbar^2/2\Im = 6.588$ keV and decoupling parameter of $a = +0.672$. With these parameters, the energy of the $11/2^+$ member is calculated to be 639 keV. From coincidence between 425.4- and a 134.9-keV γ rays (Table II), we deduce a level at 654.1 keV. This level could be the $11/2^+$ member of the $1/2^+$ band; but because we have seen only one transition deexciting this level, we have not included it in the level scheme.

Levels at 558.20 and 569.20 keV receive direct β^- population in ^{249}Cm decay, and their deexcitation pattern

suggests spin-parity of $3/2^-$ and $1/2^-$, respectively. In the α decay of ^{253}Es, the $5/2^-$, $7/2^-$, $9/2^-$, and $11/2^-$ members of this band are identified at 624.98, 606.71, 723.2, and 704.8 keV, respectively. In the γ-γ coincidence experiment, a 136.8-keV $E1$ γ ray was observed to deexcite the 558.2-keV level to the $5/2^+$ member of the $1/2^+$[400] band, which indicates negative parity for the 558.2-keV level. From the energies of the 1/2, 3/2, and 5/2 levels in the band, one calculates values for the decoupling parameter and rotational constant of $a = -1.759$ and $\hbar^2/2\Im = 4.840$ keV. Whereas unperturbed bands exhibit rotational constants of $\geqslant 6.0$ keV, the low value observed here indicates Coriolis mixing with nearby bands, a topic discussed in Sec. III B. Furthermore, the calculated energies for higher spin levels in the band show poor agreement with experiment, another sign of Coriolis mixing.

The 643.0- and 661.3-keV levels receive direct β^- population suggesting that these states have spins of either 1/2 or 3/2. The decay pattern indicates spin 1/2 for the 643.0-keV level and spin 3/2 for the 661.3-keV level. The $5/2^-$ member of this band is identified at 709.1 keV in the α decay of ^{253}Es. From these energies, the decoupling parameter is determined to be $a = -0.214$ and the rotational constant $\hbar^2/2\Im = 7.84$ keV. It is worth noting that for the six rotational bands in ^{249}Bk discussed so far, there is a direct correspondence with levels identified in ^{251}Bk from a study of ^{251}Cm β^- decay [16].

In the γ singles spectrum, shown in Fig. 3, we observe two strong γ rays of energy 1040.15 and 1075.05 keV, one of which could possibly be associated with the decay of the $9/2^+$[624] Nilsson state. The $13/2^+$ member of this band was identified in the ^{248}Cm(α, t) reaction at 1229 keV [4]. A more

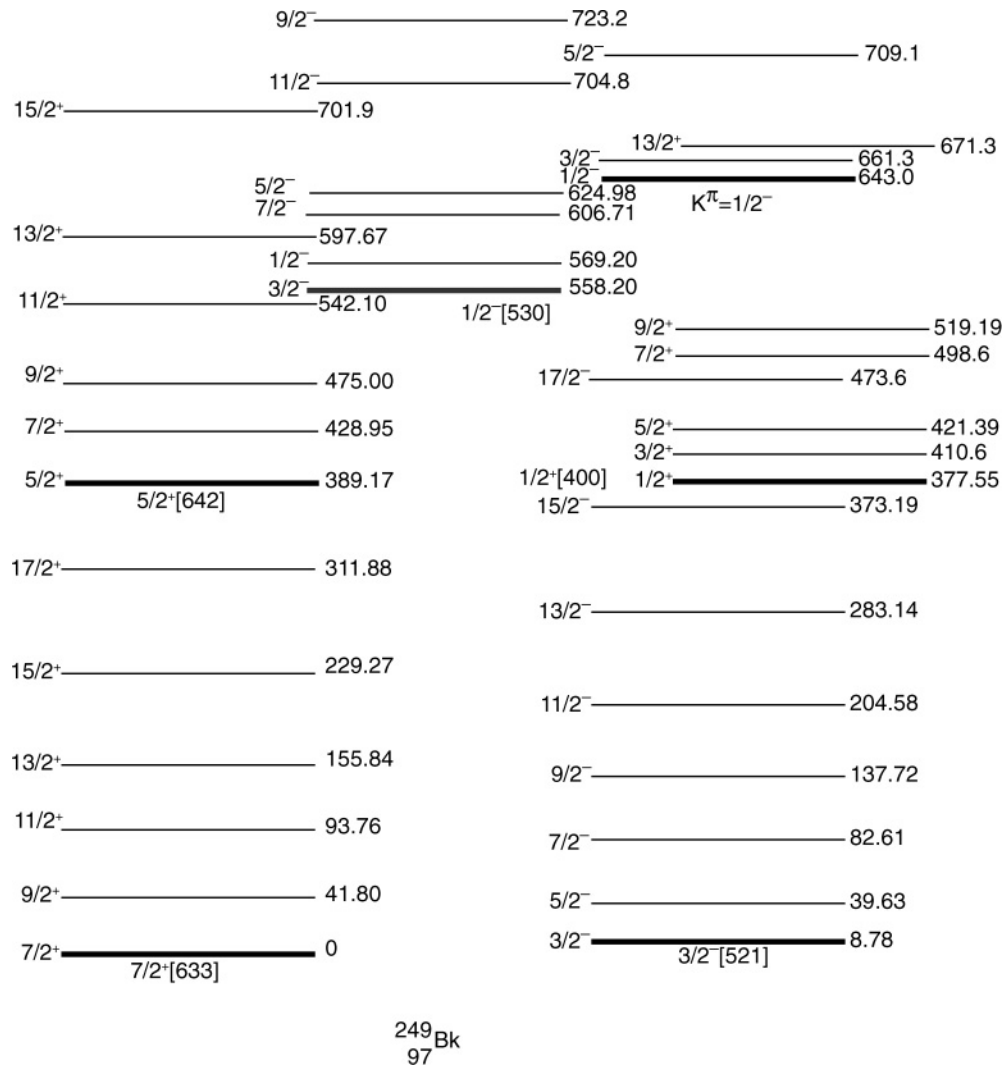FIG. 7. Energy levels of ^{249}Bk determined from the study of ^{253}Es α decay. Most of the levels were known from previous studies. Bandheads are shown by thicker lines, and all energies are in keV. Nilsson configuration, $K^{\pi}[Nn_z\Lambda]$, is also given. The 643.0-keV level has a mixed configuration of $1/2^-[521]$, $1/2^-[530]$, and $1/2^-$ collective components.

precise energy for this level was measured to be 1225 keV in the ^{248}Cm(^{3}He, d) reaction [5]. If we place the bandhead at 1040.2 keV, we obtain a rotational constant of $\hbar^2/2\Im = 7.7$ keV, which is higher than the typical value of 6.0–6.5 keV. On the other hand, with the 1075.1-keV state as the $9/2^+$ member, a reasonable value of $\hbar^2/2\Im = 6.25$ keV is derived. With this rotational constant, we calculate the energy of the $11/2^+$ member as 1143.9 keV, in close correspondence with the observed 1143.8-keV level with the expected properties for the $11/2^+$ level (shown in Fig. 9). We observe the decay of the 1075.1-keV level to the $7/2^+$ and $11/2^+$ members of the ground-state band. The energy of the transition to the $9/2^+$ member of the ground-state band is calculated to be 1033.3 keV, which falls under the intense 1031.85-keV peak of ^{250}Bk. We have determined the ratio of the intensities of the 1031.85- and 989.13-keV γ rays of ^{250}Bk in a spectrum measured soon after chemical separation in May 2003 and in another spectrum measured in September 2003, when the ^{253}Es activity had decayed by a factor of 100. The $I_{1031.85}/I_{989.13}$ ratio

was found to be $\sim$4% larger in the May spectrum, compared to that measured in September. From the excess counts in the 1031.85-keV peak of the May spectrum, we determine the intensity of the 1033.3-keV γ ray to be $\sim$1.0 × 10^{-6}% per ^{253}Es α decay.

The 1040.15- and 998.3-keV γ rays could be associated with either the decay of a 1040.2-keV level or the decay of 1133.8- and 1227.7-keV levels. We prefer the latter choice because the energies of the proposed levels agree with the values calculated with a rotational constant of $\hbar^2/2\Im = 6.15$ keV for the 13/2 and 15/2 members of the band.

A level at 672.9 keV (Fig. 9) was deduced from the observation of 672.8- and 664.0-keV (672.9→8.78) γ rays in the singles spectrum. Coincidence relationships, given in Table II and Fig. 4, establish the spin of the 672.9-keV level as 5/2. Coincident γ rays of 227.0 and 261.7 keV establish levels at 899.9 and 934.7 keV (Fig. 9). On the basis of their decay, tentative spin assignments of 3/2 and 5/2 are proposed for these levels. Coincidence data also establish levels at 624.3, 703.5,
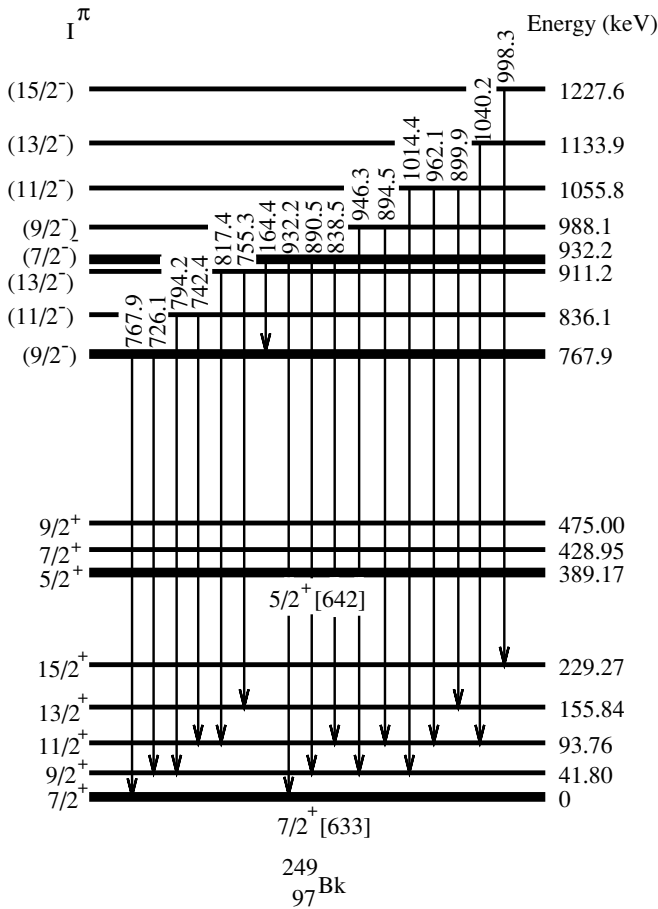
FIG. 8. Energy levels of ^{249}Bk showing the decay of high-lying states. Bandheads are shown by thicker lines. All energies are in keV. Nilsson configuration, $K^{\pi}[Nn_z\Lambda]$, is also given. Bands, with no configuration shown, are vibrational bands with configurations $\{7/2^+[633] \otimes 1^-\}9/2^-$ and $\{7/2^+[633] \otimes 0^-\}7/2^-$.

FIG. 9. Energy levels of ^{249}Bk deduced from γ singles and γ-γ coincidence data. Bandheads are shown by thicker lines. All energies are in keV. The band at 899.9 keV has a likely assignment of $\{7/2^+[633] \otimes 2^-\}3/2^-$, and the 624.3, 703.5, and 769.1 keV levels are most likely the members of the $3/2^+[651]$ band. Bands, with no configuration shown, are vibrational bands with configurations $\{7/2^+[633] \otimes 1^-\}5/2^-$, and $\{7/2^+[633] \otimes 0^+\}7/2^+$.

711.1, and 769.1 keV (Fig. 9), and these are given tentative spin assignments of 5/2, 7/2, 7/2, and 9/2, respectively, on the basis of their decay pattern.

The level at 767.9 keV (Fig. 8) decays to the 7/2 and 9/2 members of the ground-state band suggesting a spin value of 7/2 or 9/2. This level does not decay to the $5/2^+$ band at 389.2 keV, thus favoring a 9/2 spin. We have tentatively identified the 11/2 and 13/2 members of this band at 836.1 and 911.2 keV, respectively. The three levels give a rotational constant of $\hbar^2/2\Im = 6.20$ keV, which is a reasonable value in this mass region.

The level at 932.2 keV decays to the 7/2 and 9/2 members of the ground-state band. This level also decays to the 767.9-keV level by a 164.4-keV $M1$ transition (Fig. 8). Thus, this level should have the same parity as the 767.9-keV level. On the basis of its decay, the most likely spin value for this state is 7/2. The 9/2, 11/2, 13/2, and 15/2 members of this band are tentatively identified at 988.1, 1055.8, 1133.9, and 1227.6 keV, respectively. These levels fit as members of a $K = 7/2$ rotational band, and give a value of the rotational constant
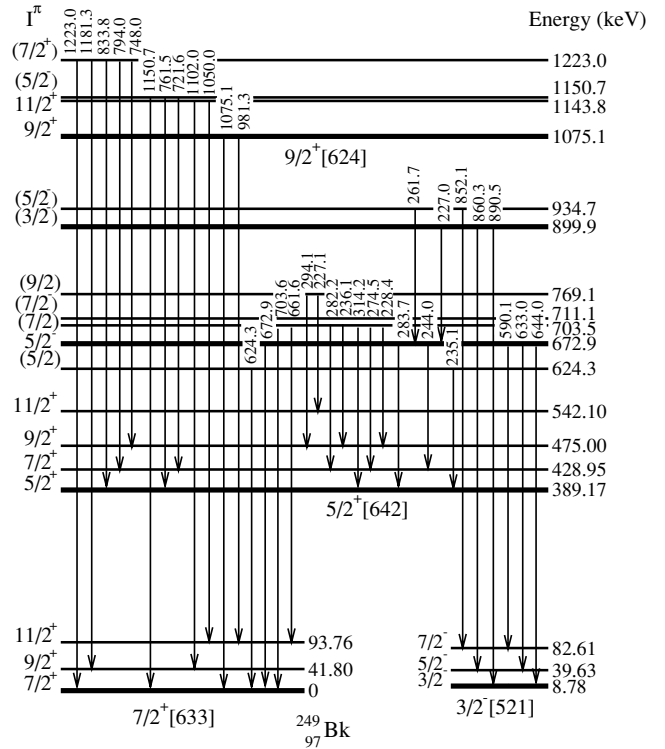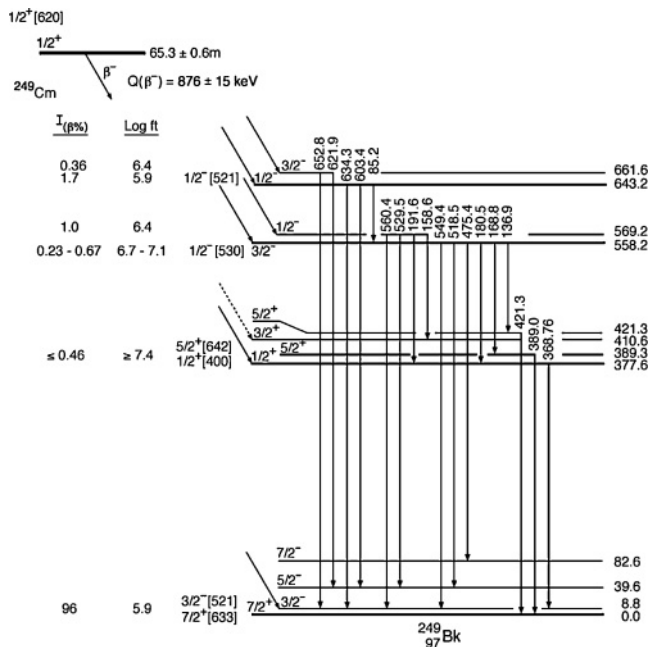

FIG. 10. Energy levels of ^{249}Bk deduced from the β^- decay of ^{249}Cm. Bandheads are shown by thicker lines. Nilsson configuration, $K^{\pi}[Nn_z\Lambda]$, is also given. All energies are in keV.

as $\hbar^2/2\Im = 6.15$ keV, similar to that of the 767.9-keV band.

The two levels at 1150.7 and 1223.0 keV decay to the ground-state band and to the $5/2^+[642]$ band. The 1223.0-keV level also deexcites to the $9/2^-$ level at 767.9 keV. The most likely spin-parity for the 1223.0-keV state is $7/2^+$, and $5/2^-$ for the 1150.7-keV state.

B. Configuration assignments

The most direct evidence for single-particle assignments comes from one-nucleon transfer reactions. Because of pairing considerations, only particle states with low values of V^2 (pair occupation probability) receive measurable cross sections in (α, t) and $(^3\text{He}, d)$ reactions. A comparison of measured cross sections of the members of a band, obtained from $^{248}\text{Cm}(\alpha, t)$ and $^{248}\text{Cm}(^3\text{He}, d)$ reactions [4,5], with the theoretical cross sections establishes the assignment of bands based on ground state, 8.78-keV, 377.55-keV, and 1075.1-keV levels to the $7/2^+[633]$, $3/2^-[521]$, $1/2^+[400]$, and $9/2^+[624]$ Nilsson orbitals, respectively. The experimental value of the decoupling parameter ($a = +0.67$) is in good agreement with the theoretical value [12] of $a = +0.59$ for the $1/2^+[400]$ orbital.

Another quantity which can be used to associate observed bandheads to intrinsic states is the α-decay hindrance factor. α-decay systematics and theoretical calculations of α-decay rates [17] have provided the following rules for α-decay hindrance factors: 1) Decays to particle states have higher hindrance factors than those to hole states; 2) decays between states with their intrinsic spins Σ parallel have lower hindrance factors than those between states with their spins antiparallel; and 3) β- and octupole-vibrational states have low hindrance factors.

The two bands at 558.2 and 643.0 keV are given $K^\pi = 1/2^-$ assignment. The values of the the rotational constant for these bands, derived from the observed level energies, indicate Coriolis mixing between these two bands and with other negative parity bands. Band mixing is also suggested by the appreciable (α, t) and $(^3\text{He}, d)$ cross sections to the members of the $1/2^-[530]$ band, which is not expected because the $1/2^-[530]$ state in ^{249}Bk is a hole state. The 1/2 and 5/2 members of the $1/2^-[530]$ band at 569 and 625 keV receive appreciable population in (α, t) and $(^3\text{He}, d)$ reactions. Also populated, but with lesser intensities, are the 1/2 and 5/2 members of the $1/2^-[521]$ band at 643 and 709 keV [5]. We have performed a Coriolis mixing calculation involving the $1/2^-[530]$, $1/2^-[521]$, and $3/2^-[521]$ bands that accurately reproduces the experimental energy for each of the 16 levels assigned to these bands. For example, the energy of the 11/2 member of the $1/2^-[530]$ band is calculated to be 704.1 keV, in excellent agreement with the proposed level at 704.8 keV. These calculations give the rotational constant and the decoupling parameter of $\hbar^2/2\Im = 6.29$ keV and $a = -1.41$ for the unperturbed $1/2^-[530]$ band and $\hbar^2/2\Im = 6.29$ keV and $a = -0.19$ for the unperturbed $1/2^-[521]$ band. This value of the decoupling parameter for the $1/2^-[530]$ band is in fair agreement with a theoretical value [12] of $a = -2.2$, while

TABLE IV. ^{253}Es α-decay hindrance factors calculated with the spin-independent theory of Preston [21]. All α energies (except for the ground-state transition) were deduced from level excitation energies, and the intensity of each α group was obtained by adding intensities of transitions deexciting that level.

Excitation energy (keV)	α energy (MeV)	Intensity (%)	Hindrance factor
0.0	6.633	89.9	1.76
672.9	5.971	$\sim 3 \times 10^{-6}$	$\sim 3 \times 10^4$
767.9	5.877	3.3×10^{-5}	830
836.1	5.810	$\sim 4 \times 10^{-6}$	$\sim 3 \times 10^3$
899.9	5.747	$\sim 3 \times 10^{-5}$	~ 170
911.2	5.736	$\sim 6 \times 10^{-6}$	~ 720
932.2	5.716	6.7×10^{-5}	51
934.7	5.713	$\sim 6 \times 10^{-6}$	~ 550
988.1	5.661	1.3×10^{-5}	126
1055.8	5.594	7.4×10^{-6}	90
1075.1	5.575	6.9×10^{-6}	74
1133.9	5.517	3.0×10^{-6}	77
1143.8	5.507	1.8×10^{-6}	112
1150.7	5.500	5.4×10^{-6}	34
1223.0	5.429	7.8×10^{-6}	8.6
1227.6	5.424	9.0×10^{-7}	70

that for the $1/2^-[521]$ band is quite different from a theoretical expectation of $a = +1.02$. The weak population of the 643.0-keV band in transfer reactions and the difference between the experimental and theoretical values of the decoupling parameter suggest that the 643.0-keV band is predominantly collective. The $1/2^-[521]$ band was identified in ^{247}Bk [18] and ^{251}Es [19] in (α, t) reactions and the cross sections are in agreement with theoretical expectations.

The relative intensities of γ rays deexciting the 672.9-keV level are very similar to the relative intensities of γ rays from the decay of the $5/2^-[523]$ state at 447.8 keV in ^{247}Bk [18]. On the basis of this similarity, we assign the $5/2^-[523]$ Nilsson state configuration to the 672.9-keV level. This assignment is further supported by the large α-decay hindrance factor ($\sim 3 \times 10^4$) given in Table IV. The level at 711.1 keV is tentatively assigned to the 7/2 member of the $5/2^-[523]$ band.

The levels at 624.3, 703.5, and 769.1 keV (Fig. 9) decay mainly to the $5/2^+[642]$ band and not to the ground or the $3/2^-[521]$ band, indicating positive parity for these levels. The decay of these levels suggests spin 3/2 or 5/2 for the 624.3-keV level and spins 7/2 and 9/2 for the 703.5- and 769.1-keV levels, respectively. These states are tentatively assigned to the $3/2^+[651]$ band. The somewhat lower energy of this band could be due to its mixing with the $\{7/2^+[633] \otimes 2^+\}3/2^+$ band, which is expected to lie at ~ 1 MeV.

The pairing gap ($\sim 2\Delta$) in heavy elements is ~ 1 MeV for neutrons and somewhat larger for protons. Thus, states with excitation energies of 1 MeV or higher may correspond to three-quasiparticle states or vibrational excitations. β- and octupole-vibrational states are known [20] to have low α-decay hindrance factors. Some three-quasiparticle states

TABLE V. g_K values in ^{249}Bk. Intensity ratios were obtained from crossover and cascade γ-ray intensities, given in Table I.

Nilsson state	I_i	Intensity ratio	$|g_K - g_R|_{\text{exp}}$	$|g_K - g_R|_{\text{theory}}$	$|\delta|_{\text{exp}}$	$|\delta|_{\text{theory}}$
$7/2^+[633]$	11/2	0.09	0.78 ± 0.06	0.83	0.15	0.11
	13/2	0.18	0.84 ± 0.06		0.14	0.11
	15/2	0.33	0.81 ± 0.06		0.15	0.12
	17/2	0.42	0.91 ± 0.06		0.13	0.12
$3/2^-[521]$	7/2	0.12	1.41 ± 0.10	1.51	0.11	0.10
	9/2	0.30	1.44 ± 0.10		0.11	0.10
	11/2	0.55	1.45 ± 0.10		0.10	0.10
	13/2	0.80	1.50 ± 0.11		0.10	0.10
	15/2	1.65	1.26 ± 0.10		0.12	0.10
	17/2	1.75	1.42 ± 0.10		0.10	0.09

may have low hindrance factors as well. We have deduced the α intensities to the high-lying states by adding the intensities of γ rays and conversion electrons deexciting these levels. For conversion electron intensities of low-energy transitions, theoretical conversion coefficients for pure $M1$ multipolarity were used. The intensities of α groups, not observed in α singles spectrum, along with corresponding hindrance factors, are given in Table IV. The hindrance factors were calculated with the spin-independent theory of Preston [21] using a radius parameter of 9.404 fm. As the table shows, the lowest hindrance factor occurs to the α transition to the 1223-keV level. In the previous section, we showed that the most likely spin-parity assignment to the 1223-keV level is $7/2^+$. We, therefore, associate this level with the β-vibrational band built on the $7/2^+[633]$ state, i.e., $\{7/2^+[633] \otimes 0^+\}7/2^+$.

The bands associated with the 767.9- and 932.2-keV levels are interpreted as the 1^- and 0^- octupole vibrational bands built on the $7/2^+[633]$ ground state, i.e., $\{7/2^+[633] \otimes 1^-\}9/2^-$ and $\{7/2^+[633] \otimes 0^-\}7/2^-$. These vibrational bands lie at approximately the same energies in ^{248}Cm [22]. The 1150.7-keV level is tentatively assigned to the $\{7/2^+[633] \otimes 1^-\}5/2^-$ configuration. This state could also have some admixture of the $5/2^-[512]$ Nilsson state which is expected to lie in this energy region. It should be noted that the hindrance factor for the 768-keV level is somewhat higher than the typical values for an octupole band.

Coincidence relationships between 227.0, 261.7, 283.7, and 664.0 keV γ rays establish levels at 899.9 and 934.7 keV. We have observed the 664.0-keV γ ray in coincidence with Bk K x rays, which suggests large conversion coefficients for the 227.0 and/or 261.7 keV transition. Because a high conversion coefficient indicates $M1$ multipolarity for the 227.0 and/or 261.7 keV transition, the parity of the 899.9- and 934.7-keV levels should be the same as that of the 672.9-keV level. We interpret these two states as the 3/2 and 5/2 members of the vibrational band $\{7/2^+[633] \otimes 2^-\}3/2^-$.

We did not identify the $7/2^-[514]$ orbital which is expected to lie in the 0.5–1.0 MeV range. This state is not expected to receive measurable α population because its intrinsic spin is antiparallel to the intrinsic spin of the ^{253}Es ground state. The 9/2 member of this band is expected to have large cross section in the ^{248}Cm(α, t) and ^{248}Cm$(^3$He$, d)$ reactions, and this level was observed at 750 keV in Refs. [4,5].

C. g-factor measurement

Several members of the ground-state band and the $3/2^-[521]$ band have been identified in the present work. Using the measured cascade to crossover γ-ray branching ratios and a quadrupole moment of $Q = 12.9\,e$ b, we have deduced the $|g_K - g_R|$ values, and these are given in Table V. The average value of $|g_K - g_R|$ for the $7/2^+[633]$ band is found to be $|g_K - g_R| = 0.84 \pm 0.08$, and for the $3/2^-[521]$ band $|g_K - g_R| = 1.43 \pm 0.12$. These are in excellent agreement with the theoretical values of $|g_K - g_R| = 0.83$ and $|g_K - g_R| = 1.30$ for the $7/2^+[633]$ and $3/2^-[521]$ bands, respectively, as calculated with the single-particle wave functions of Ref. [12] using a g_R value of $g_R = 0.31$. The excellent agreement between experiment and theory indicates that wave functions are correctly calculated with the Woods-Saxon single-particle potential.

D. γ-ray branching ratio

In the absence of strong Coriolis mixing, γ-ray reduced transition probabilities from a given level to different members of a rotational band are proportional to the squares of the appropriate Clebsch-Gordan coefficients [23]. We have deduced relative values of the reduced transition probability $B(\lambda)$ from the experimental γ-ray intensities by removing their energy dependence. These values are given in Table VI along with the theoretical values. Multipolarities of all transitions in the table are assumed to be $M1$ or $E1$ depending on the selection rules. We have listed relative transition probabilities of only those transitions whose intensities do not have contribution from another transition. We have excluded transitions from the $5/2^+[642]$ band because of its strong Coriolis mixing [2] with other bands arising from the $i_{13/2}$ shell. As the table shows, the experimental values are in good agreement with the theoretical expectations, providing addition support for the K, I^π assignments to ^{249}Bk levels.

E. Comparison with theory

In Ref. [24], single-particle spacings were extracted from the experimental data on the then known levels in ^{249}Bk by removing the contributions of the pairing correlations to

TABLE VI. γ-ray reduced transition probability. Experimental values were obtained from the γ-ray intensities in Table I.

Initial level		Final level	γ-ray energy	Relative $B(\lambda)$	Relative $B(\lambda)$
Energy (keV)	K_i, I_i^π	K_f, I_f^π	(keV)	experiment	theory
624.98	1/2, 5/2$^-$	3/2, 3/2$^-$	616.1	1.0	1.0
		3/2, 5/2$^-$	585.4	11	7
		3/2, 7/2$^-$	542.3	9	7
661.3	1/2, 3/2$^-$	3/2, 3/2$^-$	652.7	1.0	1.0
		3/2, 5/2$^-$	621.7	1.7	1.5
709.1	1/2, 5/2$^-$	3/2, 5/2$^-$	669.5	1.0	1.0
		3/2, 7/2$^-$	626.5	0.85	1.0
672.9	5/2, 5/2$^-$	3/2, 3/2$^-$	664.0	1.0	1.0
		3/2, 5/2$^-$	633.0	∼0.46	0.43
		3/2, 7/2$^-$	590.1	0.28	0.07
767.9	9/2, 9/2$^-$	7/2, 7/2$^+$	767.9	1.0	1.0
		7/2, 9/2$^+$	726.1	0.21	0.23
988.1	7/2, 9/2$^-$	7/2, 9/2$^+$	946.3	1.0	1.0
		7/2, 11/2$^+$	894.5	0.79	0.66
1075.1	9/2, 9/2$^+$	7/2, 7/2$^+$	1075.1	1.0	1.0
		7/2, 9/2$^+$	∼1033	∼0.23	0.23
		7/2, 11/2$^+$	981.3	∼0.02	0.023
1143.8	9/2, 11/2$^+$	7/2, 9/2$^+$	1102.0	1.0	1.0
		7/2, 11/2$^+$	1050.0	0.32	0.41
1150.7	5/2, 5/2$^-$	5/2, 5/2$^+$	761.5	1.0	1.0
		5/2, 7/2$^+$	721.6	0.57	0.40
1223.0	7/2, 7/2$^+$	5/2, 5/2$^+$	833.8	1.0	1.0
		5/2, 7/2$^+$	794.0	0.37	0.30

the experimental energies, using a Hamiltonian containing a density-dependent pairing interaction [25]. We have fitted the shape parameters of a Woods-Saxon potential to optimize the agreement with the extracted levels. The parameters of this Woods-Saxon potential are those used to calculate the properties of superheavy elements [26]. The Woods-Saxon potential parameters used for protons are a well depth of $V_0 = -61$ MeV for the central potential; a spin-orbit potential of $V_{\text{s.o.}} = -16.75$ MeV; a radius parameter of $r_0 = 1.275$ fm for the central potential and a reduction of 5% for the radius parameter of the spin-orbit potential; and a diffusivity parameter of $a = 0.68$ fm for both the central and the spin-orbit potentials.

Using these potential parameters, we found that the shape parameters ($\nu_2 = 0.255$, $\nu_4 = 0.01$, and $\nu_6 = 0.015$) give a single-particle spectrum that agrees very well with the extracted spacings. The quadrupole, hexadecapole, and 2^6-pole deformation parameters ν_2, ν_4, and ν_6 are closely related to the Nilsson [13] deformation parameters ϵ_2, ϵ_4, and ϵ_6. An exact definition of these deformation parameters and a comparison with other shape parametrization schemes are given in the Appendix A of Ref. [12]. In Fig. 11, we compare the extracted and calculated single-particle levels. The position of the 7/2$^+$[633] level is taken as the zero of the energy scale. With the exception of the 5/2$^+$[642] level, the agreement between the extracted spacings and the Woods-Saxon level spacings is extremely good. This good agreement is part of the reason for the choice of Woods-Saxon potential parameters made in Ref. [26].

Energies of single-particle states in ^{249}Bk were also calculated by Gareev *et al.* [27] using a quasiparticle-phonon
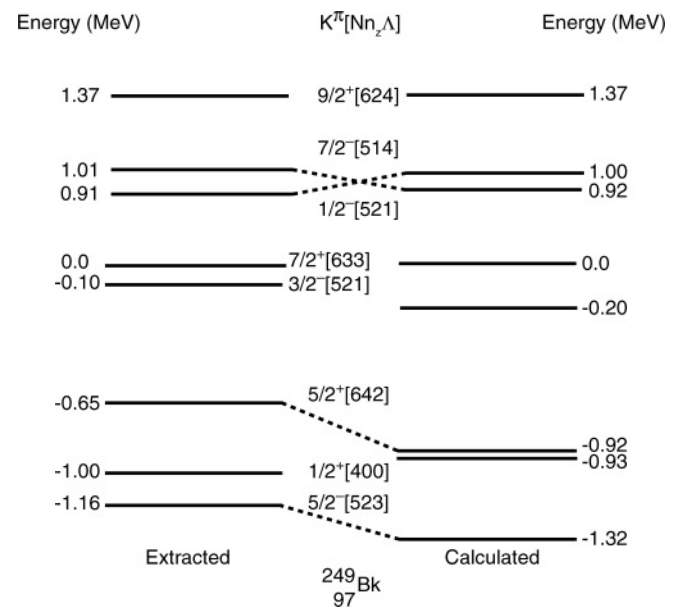

FIG. 11. Comparison of extracted level energies of ^{249}Bk with the energies calculated with a Woods-Saxon potential [26]. Extracted energies represent experimental level energies from which contributions of pairing correlations have been removed. For the Woods-Saxon potential, the deformation parameters used were $\nu_2 = 0.255$, $\nu_4 = 0.01$, and $\nu_6 = 0.015$.

interaction. Recently, proton one-quasiparticle energies were calculated by Parkhomenko and Sobiczewski [28] using the macroscopic-microscopic method without correcting for blocking effects.

F. Summary

Gamma-singles spectra of extremely pure ^{249}Cm and ^{253}Es sources have been measured with high-resolution germanium spectrometers. In ^{253}Es decay, γ rays with intensities up to $1.0 \times 10^{-6}\%$ per α decay have been identified and all γ rays with intensities above $1.0 \times 10^{-5}\%$ per α decay have been placed in a level scheme for ^{249}Bk. γ-γ coincidence measurements were performed with the GAMMASPHERE array using a ^{253}Es source. On the basis of the results of the present study and the results of previous one-proton transfer reactions, several single-particle and vibrational states have been identified. These include $7/2^+[633]$, 0.0 keV; $3/2^-[521]$, 8.78 keV; $1/2^+[400]$, 377.55 keV; $5/2^+[642]$, 389.17 keV; $1/2^-[530]$, 569.20 keV; $1/2^-[521]$, 643.0 keV; $5/2^-[523]$, 672.9 keV; and $9/2^+[624]$, 1075.1 keV. Four vibrational bands were identified at 767.9, 932.2, 1150.7, and 1223.0 keV with tentative assignments of $\{7/2^+[633] \otimes 1^-\}9/2^-$, $\{7/2^+[633] \otimes 0^-\}7/2^-$, $\{7/2^+[633] \otimes 1^-\}5/2^-$, and $\{7/2^+[633] \otimes 0^+\}7/2^+$, respectively. Data also suggest a $\{7/2^+[633] \otimes 2^-\}3/2^-$ band at 899.9 keV and the $3/2^+[651]$ band at 624.3 keV. The $7/2^-[514]$ orbital was identified in the ^{248}Cm(α, t) and ^{248}Cm(^{3}He, d) reactions. It was not observed in the present work because this state is expected to receive very low α population. The ^{248}Cm(α, t) and ^{248}Cm(^{3}He, d) reaction cross sections indicate strong mixing between the $1/2^-[530]$ and $1/2^-[521]$ states. The present study, along with previous studies of levels in ^{247}Bk [18], ^{251}Es [19,29], and ^{253}Es [30], provides a fairly complete single-proton level spectrum in the heaviest nuclides against which theoretical models used for the prediction of the properties of superheavy elements should be tested.

[1] A. Artna-Cohen, Nucl. Data Sheets **88**, 169 (1999).

[2] I. Ahmad and J. Milsted, Nucl. Phys. **A239**, 1 (1975).

[3] S. A. Baranov, V. M. Shatinskii, V. M. Kulakov, and Yu. F. Rodionov, Sov. Phys. JETP **36**, 199 (1973).

[4] J. R. Erskine, G. Kyle, R. R. Chasman, and A. M. Friedman, Phys. Rev. C **11**, 561 (1975).

[5] J. S. Boyno, H. Freiesleben, J. R. Huizenga, C. Kalbach-Cline, C. E. Bemis, and R. W. Hoff, University of Rochester Nuclear Structure Research Laboratory Annual Report, 1972 (unpublished) p. 49.

[6] I. Y. Lee, Nucl. Phys. **A520**, 641c (1990).

[7] R. Gunnink and J. B. Niday, Lawrence Livermore National laboratory Report UCRL 51016, 1971 (unpublished).

[8] I. Ahmad, E. F. Moore, J. P. Greene, C. E. Porter, and L. K. Felker, Nucl. Instr. Methods **A505**, 389 (2003).

[9] T. R. England and B. F. Rider, LA-UR-94-3106; ENDF-349, 1993 (unpublished).

[10] E. Browne and R. B. Firestone, *Table of Radioactive Isotopes* (Wiley, New York, 1986).

[11] L. A. Boatner, R. W. Reynolds, C. B. Finch, and M. M. Abraham, Phys. Lett. **A42**, 93 (1972).

[12] R. R. Chasman, I. Ahmad, A. M. Friedman, and J. R. Erskine, Rev. Mod. Phys. **49**, 833 (1977).

[13] S. G. Nilsson, K. Dan. Vidensk. Selsk. Mat. Fys. Medd. **29**, 16 (1955).

[14] R. W. Hoff, W. F. Davidson, D. D. Warner, H. G. Börner, and T. von Egidy, Phys. Rev. C **25**, 2232 (1982).

[15] T. H. Braid, R. R. Chasman, J. R. Erskine, and A. M. Friedman, Phys. Rev. C **4**, 247 (1971).

[16] R. W. Lougheed, J. F. Wild, E. K. Hulet, R. W. Hoff, and J. H. Landrum, J. Inorg. Nucl. Chem. **40**, 1865 (1978).

[17] J. K. Poggenburg, H. J. Mang, and J. O. Rasmussen, Phys. Rev. **181**, 1697 (1969).

[18] I. Ahmad, S. W. Yates, R. K. Sjoblom, and A. M. Friedman, Phys. Rev. C **20**, 290 (1979).

[19] I. Ahmad, R. K. Sjoblom, A. M. Friedman, and S. W. Yates, Phys. Rev. C **17**, 2163 (1978).

[20] S. Bjørnholm, M. Lederer, F. Asaro, and I. Perlman, Phys. Rev. **130**, 2000 (1963).

[21] M. A. Preston, Phys. Rev. **71**, 865 (1947).

[22] S. W. Yates, A. M. Friedman, and I. Ahmad, Phys. Rev. C **12**, 795 (1975).

[23] G. Alaga, K. Adler, A. Bohr, and B. R. Mottelson, K. Dan. Vidensk. Selsk. Mat. Fys. Medd. **29**, 5 (1955).

[24] R. R. Chasman, in *Proceedings of the International Symposium on Superheavy Elements*, edited by M. K. Lodhi (Pergamon Press, New York, 1978), p. 363.

[25] R. R. Chasman, Phys. Rev. C **14**, 1935 (1976).

[26] R. R. Chasman and I. Ahmad, Phys. Lett. **B392**, 255 (1997).

[27] F. A. Gareev, S. P. Ivanova, L. A. Malov, and V. G. Soloviev, Nucl. Phys. **A171**, 134 (1971).

[28] A. Parkhomenko and A. Sobiczewski, Acta Phys. Pol. B **35**, 2447 (2004).

[29] I. Ahmad, R. R. Chasman, and P. R. Fields, Phys. Rev. C **61**, 044301 (2000).

[30] K. J. Moody, R. W. Lougheed, J. F. Wild, R. J. Dougan, E. K. Hulet, R. W. Hoff, C. M. Henderson, R. J. Dupzyk, R. L. Hahn, K. Sümmerer, G. D. O'Kelly, and G. R. Bethune *et al.*, Nucl. Phys. **A563**, 21 (1993).